

# Experimental Study on Viscoelastic Behavior of Sedimentary Rock under Dynamic Loading

L. F. Fan · F. Ren · G. W. Ma

Received: 9 September 2011 / Accepted: 19 October 2011 / Published online: 5 November 2011  
© Springer-Verlag 2011

**Keywords** Sedimentary rock · Dynamic viscoelastic model · Experimental study · Pressure bar · Stress wave propagation

## 1 Introduction

Rocks with micro defects do not always behave elastically but sometimes viscoelastically under dynamic loading. Attenuation and dissipation occur when stress wave propagates through an intact rock with micro defects, which cannot be described using traditional elastic rock models (Jaeger et al. 2007). A proper viscoelastic model of rocks is thus important once the stress wave propagation caused by earthquakes, blast, and impact forces is under concern.

A variety of equipments have been used to obtain the dynamic properties of rocks, for example, drop towers, Split Hopkinson Pressure Bars (SHPB), spalling and flyer plates (ASM Int 2000). Among these set-ups, the SHPB has been widely used to test the rock dynamic strength, rock fracture, and fragmentation for their easy operation, good repeatability, and accurate results (Li et al. 2005; Li and Ma 2009; Zhou et al. 2010). However, most of these dynamic experiments were conducted with the aims of investigating the strain rate effect and rock failure behavior. The pre-failure behavior of defected rocks under

dynamic conditions is still not clear. Although some viscoelastic constitutive models have been introduced in analyzing stress wave amplitude attenuation, waveform dissipation (Pyrak-Nolte et al. 1990; Jaeger et al. 2007; Li et al. 2010), and mechanical energy dissipation (Perino et al. 2010) in jointed rock mass, these viscoelastic models were mainly proposed for the consideration of the joint effect in jointed rock mass. There still lacks an effective method to determine the viscosity and parameters in the theoretical models for rocks with micro defects.

The present technical note introduces an experimental method to determine the viscoelastic behavior of a sedimentary rock. It is found that a modified three-element viscoelastic model can best fit the experimental results. The wave propagation coefficient (wave attenuation coefficient and wave number) of the sedimentary rock are determined. The frequency dependence of the viscoelastic storage modulus and loss modulus is obtained. Discussions of the rock viscosity and its effect on stress wave propagations in the sedimentary rock are performed.

## 2 Dynamic Test of Sedimentary Rock

A series of impact tests as shown in Fig. 1 were carried out to investigate the viscoelastic behavior of a sedimentary rock. The sedimentary rock bar was cored from an underground cavern construction site with a length of 129.80 cm, a diameter of 4.49 cm and a density of 2,681 kg/m<sup>3</sup>. The integrity and homogeneity of the sedimentary rock bar were carefully examined and the end surface of the bar was grinded by a grinding machine to make a flat free end. A steel pendulum hammer was used to generate a longitudinal pulse and the intensity of the pulse load could be adjusted by changing the swinging angle of

---

L. F. Fan  
School of Civil and Environmental Engineering,  
Nanyang Technological University, Singapore 639798,  
Singapore

F. Ren · G. W. Ma (✉)  
School of Civil and Resource Engineering,  
The University of Western Australia,  
Crawley, WA 6009, Australia  
e-mail: ma@civil.uwa.edu.au

the hammer. A pair of rollers was designed to support the sedimentary rock bar in order to eliminate the friction effect from the supports. The longitudinal strain waves were measured by using a pair of diametrically opposite strain gauges located at the middle of the bar as shown in Fig. 1. The strain time history was recorded at a time rate of  $1.00 \times 10^7 \text{ s}^{-1}$  (time resolution of  $1.00 \times 10^{-7} \text{ s}$ ), which gave sufficient data points with sufficient accuracy to perform a discrete Fourier transformation.

According to one-dimensional stress wave propagation theory (Lundberg and Blanc 1988; Bacon 1998; Benatar et al. 2003), once an impact is applied to the boundary at  $x = 0$ , the attenuation coefficient  $\alpha(\omega)$  and the wave number  $k(\omega)$  can be deduced from the Fourier transformation of measured strain as a function of  $x$  and  $\omega$  as

$$\alpha(\omega) = -\text{Re} \left[ \ln \frac{\left( \frac{\mathbb{F}(|\varepsilon_2|)}{\mathbb{F}(|\varepsilon_1|)} \right)}{l} \right] \tag{1}$$

and

$$k(\omega) = -\text{Im} \left[ \ln \frac{\left( \frac{\mathbb{F}(|\varepsilon_2|)}{\mathbb{F}(|\varepsilon_1|)} \right)}{l} \right] \tag{2}$$

respectively, where  $\omega$  is the angular frequency of a harmonic component wave after Fourier transformation,  $\varepsilon_1$  is

the first measured strain pulse in the increasing  $x$  direction produced by the pendulum and  $\varepsilon_2$  is the second measured strain pulse in the decreasing  $x$  direction which is reflected from the free surface at the distal end,  $l$  denotes the wave traveling distance between these two pulses,  $\mathbb{F}$  denotes the treatment of applying the Fourier transformation,  $Re$  and  $Im$  denote the real and imaginary parts of the complex expression, respectively.

Consequently, the storage modulus  $E'(\omega)$  and the loss modulus  $E''(\omega)$  of the rock are determined from Eqs. 1 and 2 as

$$E'(\omega) = \frac{\rho\omega^2(k^2 - \alpha^2)}{(k^2 + \alpha^2)^2} \tag{3}$$

and

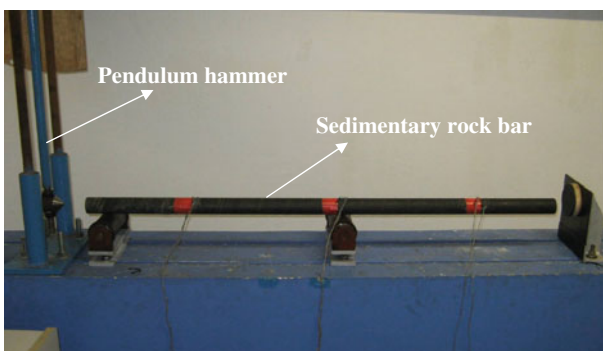
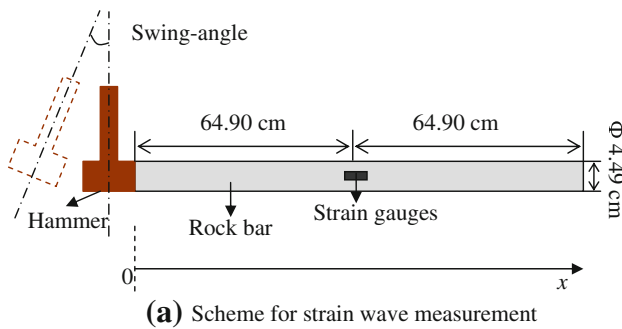
$$E''(\omega) = \frac{2\rho\omega^2k\alpha}{(k^2 + \alpha^2)^2} \tag{4}$$

respectively, where  $\rho$  denotes the rock density (Lundberg and Blanc 1988; Bacon 1998; Benatar et al. 2003).

Equations 1–4 introduce the method to determine the viscoelastic parameters experimentally. The attenuation coefficient  $\alpha(\omega)$ , the wave number  $k(\omega)$ , the storage modulus  $E'(\omega)$ , and the loss modulus  $E''(\omega)$  are derived from the measured strain signals. The following Sect. 3 shows that a modified three-element viscoelastic model can fit the experimental results well and Sect. 4 discusses the effect of the viscoelastic behavior on stress wave propagations.

### 3 A Modified Three-Element Viscoelastic Model

A modified three-element viscoelastic model is used to simulate the viscoelastic behavior of the sedimentary rock. The model as shown in Fig. 2 is an auxiliary spring in parallel with a modified Maxwell element. The modified Maxwell element consists of a spring with a frequency dependent elastic constant  $E_v(\omega)$  and a dashpot with a frequency dependent damping ratio  $\eta_v(\omega)$ , which is used to describe the frequency dependent viscosity of rock. If the



(b) Experimental setup

Fig. 1 Experimental setup for impact test

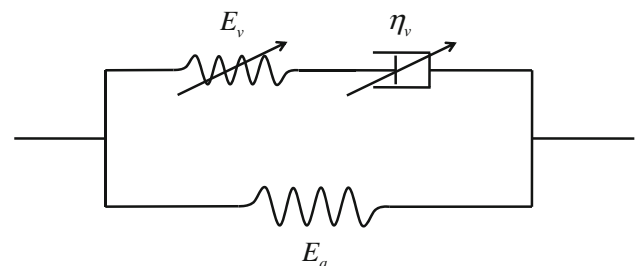


Fig. 2 Modified three-element viscoelastic model

strain-rate is sufficiently small, such as under fully relaxation, the Maxwell element term can be neglected. In that case, the present model is degraded to the spring model with an elastic constant  $E_a$ , which is the static elastic modulus of the rock.

The constitutive equation of the present model can be written as

$$E_v \sigma(x, t) + \eta_v \frac{\partial \sigma(x, t)}{\partial t} = E_a E_v \varepsilon(x, t) + (E_a + E_v) \eta_v \frac{\partial \varepsilon(x, t)}{\partial t} \tag{5}$$

where  $t$  is the time,  $\sigma(x, t)$  and  $\varepsilon(x, t)$  denotes stress and strain in the time domain, respectively.

A Fourier transformation is applied to Eq. 5 to obtain the constitutive equation in the frequency domain, Eq. 5 is changed to

$$(E_v + i\omega\eta_v)\tilde{\sigma} = [E_a E_v + i\omega(E_a + E_v)\eta_v]\tilde{\varepsilon} \tag{6}$$

where  $\tilde{\sigma}(x, \omega)$  and  $\tilde{\varepsilon}(x, \omega)$  denote the Fourier transformation of stress and strain, respectively.

Therefore, the complex dynamic modulus of the present model is derived from Eq. 6 as

$$E^*(\omega) = \frac{\tilde{\sigma}(x, \omega)}{\tilde{\varepsilon}(x, \omega)} = E_a + \frac{\omega^2 \tau_v^2}{1 + \omega^2 \tau_v^2} E_v + i \frac{\omega \tau_v}{1 + \omega^2 \tau_v^2} E_v \tag{7}$$

The retardation time of the Maxwell element is defined as  $\tau_v = \eta_v / E_v$ .

Thus, the relations between the real and imaginary parts of the rock dynamic modulus versus the material constants are given by

$$E'(\omega) = E_a + \frac{\omega^2 \tau_v^2}{1 + \omega^2 \tau_v^2} E_v \tag{8}$$

and

$$E''(\omega) = \frac{\omega \tau_v}{1 + \omega^2 \tau_v^2} E_v \tag{9}$$

respectively, where  $E'(\omega)$  and  $E''(\omega)$  are, respectively, the dynamic storage modulus and the dynamic loss modulus and they should equate to the dynamic moduli obtained by experiments as given in Eqs. 3 and 4, respectively.

It is noticed from Eqs. 1–4, 8 and 9 that  $\alpha(\omega)$ ,  $k(\omega)$ ,  $E'(\omega)$ , and  $E''(\omega)$  all depend on the component wave frequency  $\omega$  as well as the material constants  $E_a$ ,  $E_v$ ,  $\eta_v$ .

The wave number  $k(\omega)$  is a monotonic continuous function of the frequency. However, it is observed from Eq. 2 that the imaginary part of the complex expression is generally calculated in the range from 0 to  $2\pi$ , which makes the function discontinuous to the frequency during numerical calculation. This error can be corrected by adding multiples of  $\pm 2\pi$  when absolute jumps occur (Bacon 1998).

## 4 Results and Discussions

### 4.1 Attenuation Coefficient

The attenuation coefficient and wave number versus the component wave frequency are shown in Fig. 3. It can be observed that both the attenuation coefficient and the wave number are frequency dependent. The attenuation coefficient increases with the increase of the component wave frequency, which reveals that the component wave with a higher frequency will attenuate much faster than those with lower frequencies. Because the stress wave can always be regarded as the sum of a series of harmonic component waves with different frequencies from low to high, it is resulted that a stress wave dissipates when it propagates through a viscoelastic sedimentary rock bar.

It is also seen from Fig. 3 that the wave number is approximately proportional to the frequency. The phase velocity of a stress wave can be defined as the ratio of the wave frequency to the wave number. Therefore, it is obtained that the stress wave attenuation is highly frequency dependent, while the phase velocity is insensitive to the component wave frequency.

It should be mentioned the previous investigations (Kolsky 1963; Lundberg and Blanc 1988; Blanc 1993; Bacon 1998; Benatar et al. 2003; Li and Ma 2009) have showed that when the dimension of the pressure bar’s cross-section is much smaller comparing to the wavelengths involved in the disturbance, the one-dimensional wave propagation theory will be valid, and the 3D effect can be neglected. In the present work, the pressure bar has a uniform diameter of 4.49 cm, much smaller than the wavelength which is about 1.76 m. Therefore, the wave attenuation was caused by the viscosity of the material rather than the lateral geometrical effect.

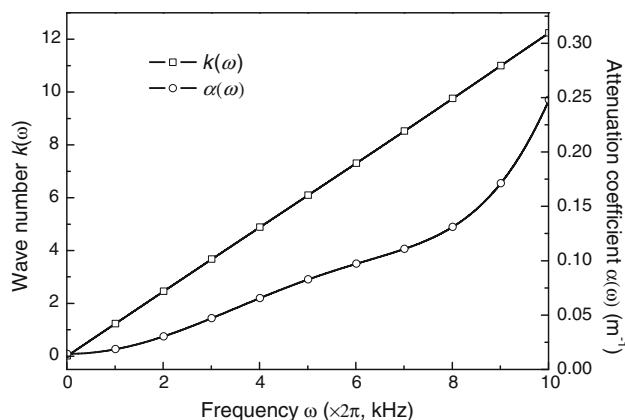


Fig. 3 Relation of propagation coefficients ( $\alpha$  and  $k$ ) with frequency  $\omega$

### 4.2 Viscoelastic Moduli

The storage modulus and the loss modulus determined by Eqs. 3 and 4 were plotted in Fig. 4. It can be observed that there are three ranges for the loss modulus changing with the component wave frequency. The loss modulus increases rapidly to a maximum value of  $E''_{max} = 44.6$  GPa in the first range up to approximately 0.03 kHz and then decreases from the maximum value with increasing frequency in the second range from 0.03 to approximately 1.60 kHz. In the third range when the frequency is larger than 1.60 kHz, the loss modulus approximately keeps a constant of 2.0 GPa with differences <1%. The storage modulus is relatively small in the frequency range when the frequency is smaller than 0.03 kHz, which increases rapidly as the corresponding frequency increasing. Then it approaches a constant of about 71.6 GPa if the frequency is larger than 1.60 kHz.

It is concluded that the two moduli are very sensitive to the component wave frequency when it is less than about 1.60 kHz. Beyond this, the two moduli are less sensitive to the component wave frequency although there are still some small changes with the increase of the frequency. When the frequency is sufficiently large, the storage modulus and the loss modulus approach constants where  $E'$  is approximately 71.6 GPa and  $E''$  is about 2.0 GPa, the storage modulus is much larger than the loss modulus. Although the dynamic moduli are obtained in the frequency range from 0 to 6.50 kHz in the present experiments, their values in the higher frequency range can be extrapolated based on the varying trend as shown in Fig. 4.

### 4.3 Parameters in the Viscoelastic Model

Experimental results of  $E'(\omega)$  and  $E''(\omega)$  shown in Fig. 4 are used to derive the parameters of the modified three-element model as a function of the component wave

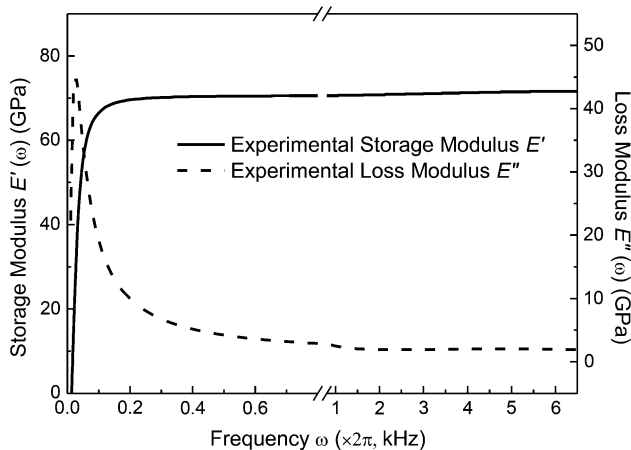


Fig. 4 Dynamic complex modulus of sedimentary rock

frequency  $\omega$ . The elastic modulus of the spring  $E_a$  in the modified three-element model is assumed to be a constant (Li et al. 2010), while  $\eta_v$  and  $E_v$  are frequency dependent. Trial values of  $E_a$ ,  $\eta_v$  and  $E_v$  were used to search for the best fitting to the experiment results, the final values of  $E_a$ ,  $\eta_v$  and  $E_v$  were determined when a negligible error was calculated which is 0.1% in the present calculation.

Figure 5 shows the relations of the parameters of  $E_v(\omega)$ ,  $\eta_v(\omega)$  versus frequency  $\omega$ , in which the elastic modulus of the spring is  $E_a = 55.8$  GPa. It is seen that both  $E_v(\omega)$  and  $\eta_v(\omega)$  are highly frequency dependent, and they decrease with the increasing component wave frequency  $\omega$ . Similar to the dynamic viscoelastic moduli in Fig. 4, it can be observed from the varying tendency of  $E_v(\omega)$ ,  $\eta_v(\omega)$  that although only the frequency range 0–6.50 kHz is calculated from the present experimental results, the parameters of the present model can be extrapolated reasonably in the higher frequency range.

### 4.4 Effect of Viscoelasticity on Stress Wave Attenuation

A transmission coefficient is defined as the ratio of the amplitude of the propagating wave over the amplitude of the incident wave to evaluate the effect of rock viscoelasticity on stress wave attenuation.

Without loss of the generality, define an incident wave with a standard single half-cycle sinusoidal function as

$$\varepsilon_{inc} = \begin{cases} I_0 \sin(2\pi \times f_0 \times t) & \text{when } 0 \leq t \leq 1/(2f_0) \\ 0 & \text{others} \end{cases} \quad (10)$$

where  $f_0$  is the frequency of the incident wave,  $I_0$  is the amplitude of the incident wave.

The relations of the transmission coefficient versus the incident wave frequency  $f_0$  and the propagation distance  $D$ , which is defined as the distance calculated between the particle velocity peaks of the incident and propagating

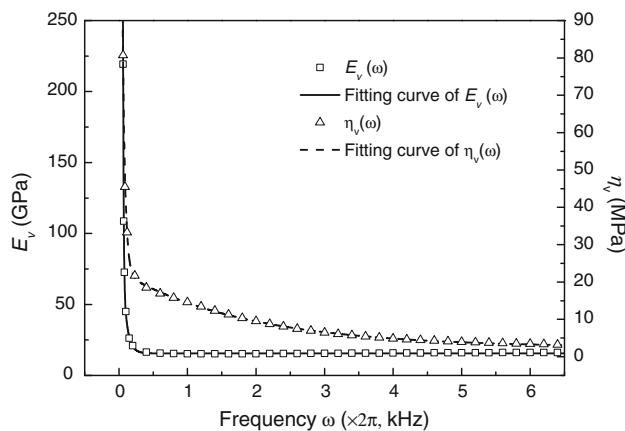
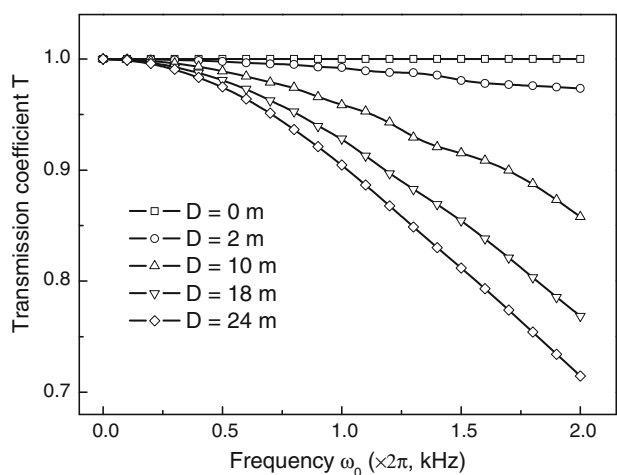


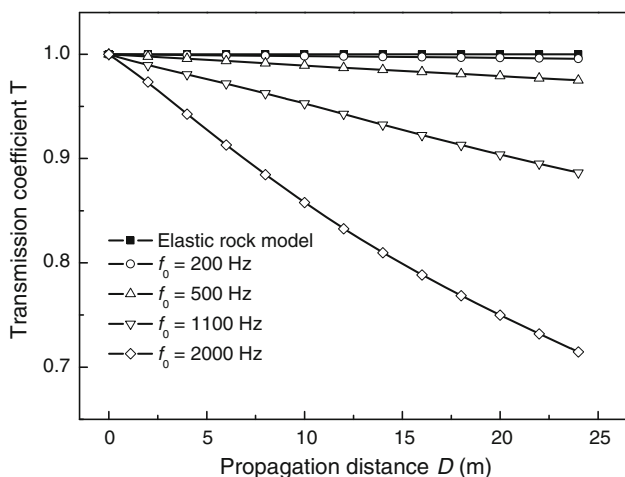
Fig. 5 Relations among parameters  $E_v(\omega)$ ,  $\eta_v(\omega)$  with frequency  $\omega$

waves, are plotted in Fig. 6. Figure 6a and b show the effect of the incident wave frequency  $f_0$  on the transmission coefficient for fixed wave propagation distances and the effect of wave propagation distance on the transmission coefficient for fixed incident wave frequencies, respectively. It is seen that the wave attenuation in the sedimentary rock not only relates to the wave propagation distance, but also highly depends on the input wave frequency.

Figure 6a shows that the transmission coefficient decreases as the incident wave frequency increase for a given wave propagation distance. The stress wave with higher frequency attenuates faster than those with lower frequencies. The transmission coefficient in Fig. 6a also verifies that the present modified three-element viscoelastic model can be properly used to describe the frequency dependent viscoelastic behavior of the sedimentary rock.



(a)  $T \sim f_0$  (for fixed  $D$ )



(b)  $T \sim D$  (for fixed  $f_0$ )

**Fig. 6** Relations of transmission coefficient  $T$  versus frequency  $f_0$  and propagation distance  $D$

Figure 6b shows that the transmission coefficient decreases as the wave propagation distance increasing for an incident wave with a given frequency. However, the decreasing rate of the transmission coefficient becomes smaller with the increase of the wave propagation distance. The transmission coefficient approaches 1 when the propagation distance becomes zero. From Fig. 6b, it is noticed again that the incident waves with higher frequencies attenuate faster. When the incident wave frequency  $f_0$  approaches zero, the transmission coefficient approaches 1, in which condition, the present three-element viscoelastic model degrades to the traditional static elastic model as a spring with the stiffness of  $E_a$ .

### 5 Conclusions

The present work experimentally investigated the dynamic viscoelastic behavior of a sedimentary rock. Impact tests on a slender rock pressure bar show that the sedimentary rock exhibits obvious viscoelastic behavior under dynamic loading. By applying one-dimensional stress wave propagation theory, the wave propagation coefficients such as the attenuation coefficient and the wave number of the sedimentary rock are determined. These wave propagation coefficients exhibit obvious frequency dependence. The modified three-element viscoelastic model used in the present study is capable in describing the frequency dependence of the viscosity under dynamic loading.

The dynamic moduli of the sedimentary rock (both storage modulus and loss modulus) are also highly frequency dependent in the smaller frequency range. The viscoelastic parameters of the modified three-element model can be regarded as constants only if the frequency is sufficiently large.

In addition, the traditional elastic rock model is a special case of the present modified three-element viscoelastic model when the wave frequency is sufficiently small. Although only the compressive stress wave with a half sinusoidal waveform was analyzed, other kinds of waves (e.g. shear wave) with other waveforms (e.g. triangular waveform, rectangular waveform) can also be adopted for similar analysis.

The present model is applicable to practical problems, such as to evaluate the peak particle velocity (PPV) attenuation law in a rock blast scenario. In principle, an incident wave with any waveform can always be regarded as the sum of harmonic component waves by using the Fourier transformation. The present modified three-element viscoelastic model determines the complex moduli by Eqs. 8 and 9 and then gives the attenuation coefficient and the wave number of a defected rock. Therefore, the corresponding transmitted harmonic component waves at any

position can be calculated. However, in a practical case when a rock mass is under consideration, the distribution of macro discontinuities such as rock joints and faults will also affect stress wave propagation significantly, the combined effect of micro defects and macro discontinuities on stress wave propagation and their application to practical cases is not discussed in this note.

## References

- ASM Int (2000) High strain rate testing, ASM handbook, vol 8. Mechanical Testing and Evaluation, Materials Park, OH, pp 939–1269
- Bacon C (1998) An experimental method for considering dispersion and attenuation in a viscoelastic Hopkinson bar. *Exp Mech* 38(4):242–249
- Benatar A, Rittel D, Yarin AL (2003) Theoretical and experimental analysis of longitudinal wave propagation in cylindrical viscoelastic rods. *J Mech Phys Solids* 51:1413–1431
- Blanc RH (1993) Transient wave propagation methods for determining the viscoelastic properties of solids. *J Appl Mech Trans ASME* 60:763–768
- Jaeger JC, Cook NGW, Zimmerman RW (2007) *Fundamentals of rock mechanics*. Blackwell Publ, Malden
- Kolsky H (1963) *Stress waves in solids*. Dover, New York
- Li JC, Ma GW (2009) Experimental study of stress wave propagation across a filled rock joint. *Int J Rock Mech Min Sci* 46:471–478
- Li JC, Ma GW, Zhao J (2010) An equivalent viscoelastic model for rock mass with parallel joints. *J Geophys Res* 115:B03305
- Li XB, Lok TS, Zhao J (2005) Dynamic characteristics of granite subjected to intermediate loading rate. *Rock Mech Rock Eng* 38(1):21–39
- Lundberg B, Blanc RH (1988) Determination of mechanical material properties from the two-point response of an impacted linearly viscoelastic rod specimen. *J Sound Vibr* 126(1):97–108
- Perino A, Zhu JB, Li JC, Barla G, Zhao J (2010) Theoretical methods for wave propagation across jointed rock masses. *Rock Mech Rock Eng* 43:799–809
- Pyrak-Nolte LJ, Myer LR, Cook NGW (1990) Anisotropy in seismic velocities and amplitudes from multiple parallel fractures. *J Geophys Res* 95(B7):11345–11358
- Zhou Z, Li X, Ye Z, Liu K (2010) Obtaining constitutive relationship for rate-dependent rock in SHPB tests. *Rock Mech Rock Eng* 43:697–706